The Influence of the Magnetic Field on the Deposition Rate and Ionized Flux Fraction in the HiPIMS Discharge

J. T. Guðmundsson[1,2], H. Hajihoseini[2,3], Martin Čada[4], Zdeněk Hubička[4], Nils Brenning[1,3,5], Michael A Raadu[1], Tiberiu Minea[3], and Daniel Lundin[3,5,6]

[1] Department of Space and Plasma Physics, KTH Royal Institute of Technology, Stockholm, Sweden
[2] Science Institute, University of Iceland, Reykjavik, Iceland
[3] Laboratoire de Physique des Gaz et Plasmas - LPGP, CNRS, Université Paris-Sud, Orsay, France
[4] Institute of Physics v. v. i., Academy of Sciences of the Czech Republic, Prague, Czech Republic
[5] Plasma and Coatings Physics, IFM-Materials Physics, Linköping University, Sweden
[6] Ionautics AB, Linköping, Sweden

AVS International Symposium & Exibition, Columbus, Ohio
October 21., 2019

Introduction – Magnetron sputtering

- Magnetron sputtering has been a highly sucessfull technique that is essential in a number of industrial applications

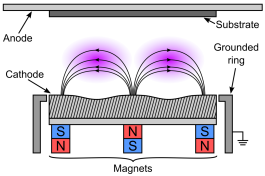

- Conventional dc magnetron sputtering (dcMS) suffers from a low degree of ionization of the sputtered material
- High power impulse magnetron sputtering (HiPIMS) provides a highly ionized material flux, while being compatible with conventional magnetron sputtering deposition systems

Introduction – HiPIMS

- High ionization of sputtered material requires very high density plasma
- In a conventional dc magnetron sputtering discharge the power density (plasma density) is limited by the thermal load on the target
- High power pulsed magnetron sputtering (HPPMS)
- In a HiPIMS discharge a high power pulse is supplied for a short period
    - low frequency
    - low duty cycle
    - low average power

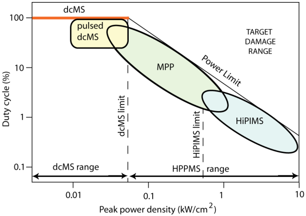

Gudmundsson et al. (2012) JVSTA **30** 030801

- Power density limits
  $p_t = 0.05$ kW/cm^2 dcMS limit
  $p_t = 0.5$ kW/cm^2 HiPIMS limit

Introduction – fraction of ionization

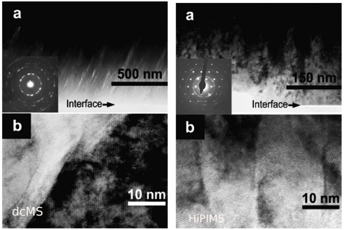

dc magnetron HiPIMS

After Alami et al. (2005) JVSTA, **23** 278

- In HiPIMS deposition, the high fraction of ionization of the sputtered species has been shown to lead to
  - the growth of smooth and dense films
  - enable control over their phase composition and microstructure
  - enhance mechanical and optical properties
  - improving film adhesion
  - enabling deposition of uniform films on complex-shaped substrates
- For optimization of HiPIMS thin film deposition processes, quantification and control of the fraction of ionization of the sputtered species are for obvious reasons key requirements

Introduction – fraction of ionization

- The effect of ionization fraction on the epitaxial growth of Cu film on Cu(111) substrate explored using Molecular Dynamics simulation
- Three deposition methods
  - thermal evaporation, fully neutral
  - dcMS, 50 % ionized
  - HiPIMS, 100 % ionized
- Higher ionization fraction of the deposition flux leads to smoother surfaces by two major mechanisms
  - decreasing clustering in the vapor phase
  - bicollision of high energy ions at the film surface that prevents island growth to become dominant

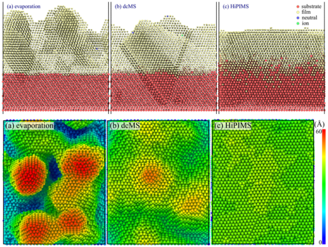

After Kateb et al. (2019) JVSTA, **37** 031306

Fraction of ionization

Fraction of ionization

- Quantification and control of the fraction of ionization of the sputtered species are crucial in magnetron sputtering
- We distinguish between three approaches to describe the degree (or fraction) of ionization
  - the ionized flux fraction

$$F_{\mathrm{flux}} = \frac{\Gamma_{\mathrm{i}}}{\Gamma_{\mathrm{i}} + \Gamma_{\mathrm{n}}}$$

  - the ionized density fraction

$$F_{\mathrm{density}} = \frac{n_{\mathrm{i}}}{n_{\mathrm{i}} + n_{\mathrm{n}}}$$

  - the fraction α of the sputtered metal atoms that become ionized in the plasma (probability of ionization)

Fraction of ionization

- There have been conflicting reports on the ionized flux fraction F_{flux}
  - 70 % for Cu (Kouznetsov et al., 1999)
  - 40 % for $Ti_{0.5}Al_{0.5}$ (Macak et al., 2000)
  - 9.5 % for Al (DeKoven et al., 2003)
  - 4.5 % for C (DeKoven et al., 2003)
  - 20 – 60 % for Ti (Kubart et al., 2014)
  - 20 – 68 % for Ti (Lundin et al., 2015)
- The degree of ionization F_{density}
  - 90 % for Ti (Bohlmark et al., 2005)
- The ionization flux fraction depends on applied power, working gas, target material, discharge current density, pulse frequency and pulse length and the magnetic field strength

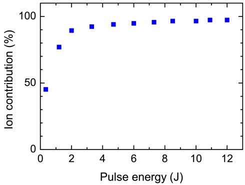

From Bohlmark et al. (2005) JVSTA **23** 18

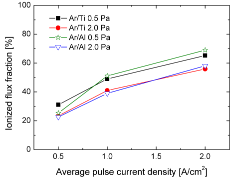

From Lundin et al. (2015) PSST **24** 035018

Fraction of ionization

- There have been a number of reports demonstrating the lower deposition rate in HiPIMS when compared to dcMS operated at the same average power (Helmersson et al., 2006; Anders, 2010).
- Samuelsson et al. (2010) compared the deposition rates from eight metal targets (Ti, Cr, Zr, Al, Cu, Ta, Pt, Ag) in pure Ar for both dcMS and HiPIMS discharges applying the same average power
- They observed that the HiPIMS deposition rates were in the range of 30 – 85% of the dcMS rates depending on target material.

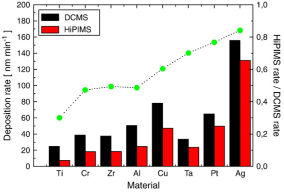

From Samuelsson et al. (2010) SCT **202** 591

Influence of magnetic field

Influence of magnetic field – Deposition rate

- The magnetic field distribution above the target for seven different magnet configurations: C0E0, C5E5 and C10E10, C0E5, C0E10, C5E0, and C10E
- For the configurations investigated, it was found that a magnetic null point was always present, which means that all configurations ware categorized as unbalanced type II
- The magnetic null was used as a measure of the degree of balancing and is in the range 43–74 mm from the target surface above the target center

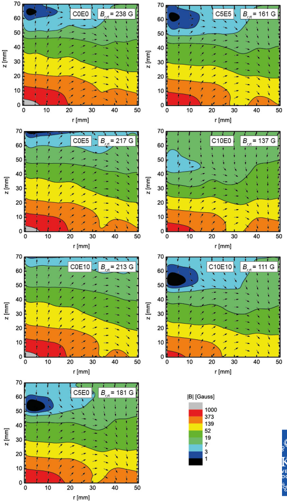

Influence of magnetic field – Deposition rate

- The HiPIMS discharge current and voltage waveforms recorded for various magnetic field configurations
    - (a) the discharge voltage in fixed voltage mode
    - (b) the discharge current in fixed voltage mode
    - (c) discharge current in fixed peak current mode
- The Ar pressure was set to 1 Pa
- In all cases the pulse width was 100 μs at an average power of 300 W

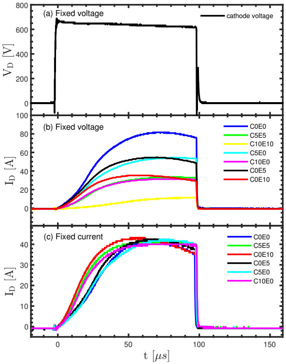

From Hajihoseini et al. (2019) *Plasma* **2** 201

Influence of magnetic field – Deposition rate

- The Ti deposition rate and the ionized flux fraction are measured using a gridless ion meter (m-QCM)
- The gridless ion meter gives the absolute value of the ionized flux fractions of the sputtered material
- The ion meter is mounted on the probe holder which can be moved around within the chamber

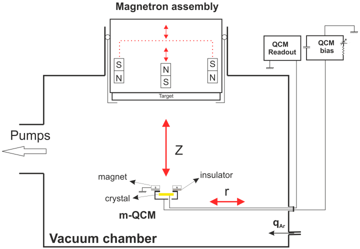

From Hajihoseini et al. (2019) *Plasma* **2** 201

Kubart et al. (2014) *SCT* **238** 152

Lundin et al. (2015) *PSST* **24** 035018

Influence of magnetic field – Deposition rate

- The Ti deposition rate from both dcMS and HiPIMS discharges operated in fixed voltage mode and fixed current mode using various magnetic field configurations measured at 70 mm axial distance over center of cathode
- The magnet configurations on the $x-$axis are ordered from high $|\mathbf{B}|$ at the left to low $|\mathbf{B}|$ on the right
- The recorded $|B_{r,\mathrm{rt}}|$ value above the race track is used as a measure of $|\mathbf{B}|$

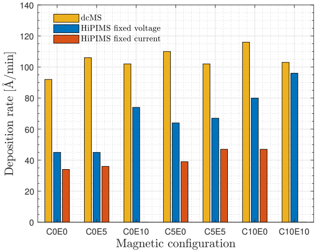

From Hajihoseini et al. (2019) *Plasma* **2** 201

Influence of magnetic field – Deposition rate

- The Ti deposition rate recorded at substrate position using the gridless ion meter (m-QCM)
  - **dcMS**
    +10% with decreasing |**B**|
    (but no obvious trend)
  - **HiPIMS fixed voltage**
    +110% with decreasing |**B**|
  - **HiPIMS fixed peak current**
    +40% with decreasing |**B**|
- In HiPIMS operation the deposition rate increases with decreasing |**B**|

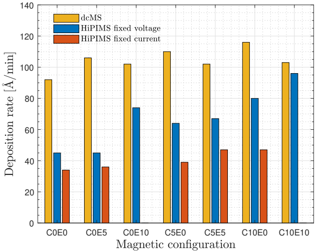

From Hajihoseini et al. (2019) *Plasma* **2** 201

Influence of magnetic field – Ionized flux fraction

- The Ti ionized flux fraction in a HiPIMS discharge using various magnet configurations measured at 70 mm axial distance over the center of the cathode
- The magnet configurations on the $x-$axis are ordered from high $|\mathbf{B}|$ at the left to low $|\mathbf{B}|$ on the right
- The recorded $|B_{r,\mathrm{rt}}|$ value above the race track is used as a measure of $|\mathbf{B}|$

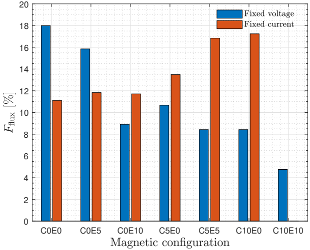

From Hajihoseini et al. (2019) *Plasma* **2** 201

Influence of magnetic field – Ionized flux fraction

- Ionized flux fraction recorded
  - **dcMS**
    Always around 0 %
    (Kubart et al., 2014)
  - **HiPIMS fixed voltage**
    -75% with decreasing $|\mathbf{B}|$
  - **HiPIMS fixed peak current**
    $+50\%$ with decreasing $|\mathbf{B}|$
- The ionized flux fraction decreases with decreasing $|\mathbf{B}|$ when the HiPIMS discharge is operated in fixed voltage mode but increases in fixed peak current mode
- Opposing trends

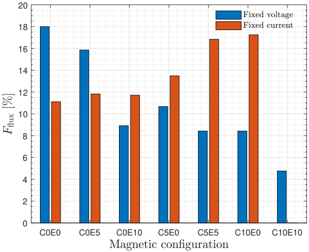

From Hajihoseini et al. (2019) *Plasma* **2** 201

Influence of magnetic field – α_t and β_t

- We relate the measured quantities deposition rate and the ionized flux fraction to the parameters
  - α_t – ionization probability
  - β_t – back-attraction probability
- Let us call the total flux (atoms/s) of atoms sputtered from the target Γ_0 and the flux of sputtered species (ions and neutrals) that leave the ionization region (IR) towards the diffusion region (DR) Γ_DR
- The useful fraction of the sputtered species becomes

$$F_\mathrm{DR} = \frac{\Gamma_\mathrm{DR}}{\Gamma_0} = (1 - \alpha_\mathrm{t}\beta_\mathrm{t})$$

- A reduced fraction of the sputtered species reaching the substrate when the ionization of the sputtered material increases
- Recall that the main drawback using HiPIMS is the low deposition rate

Influence of magnetic field – α_t and β_t

- A relationship between the ionization flux fraction F_flux and the parameters α_t and β_t has been derived from the pathway model (Vlček and Burcalová, 2010; Butler et al., 2018)

$$F_\mathrm{flux} = \frac{\Gamma_\mathrm{DR,ions}}{\Gamma_\mathrm{DR}} = \frac{\Gamma_0\alpha_\mathrm{t}(1-\beta_\mathrm{t})}{\Gamma_0(1-\alpha_\mathrm{t}\beta_\mathrm{t})} = \frac{\alpha_\mathrm{t}(1-\beta_\mathrm{t})}{(1-\alpha_\mathrm{t}\beta_\mathrm{t})}$$

  where no additional ionization of the sputtered material in the diffusion region is assumed
- Our goal is to assess how much $|\mathbf{B}|$ and the magnetic field structure influence α_t and β_t, repectively

Influence of magnetic field – α_t and β_t

- A graph that shows F_DR on the horizontal axis, and F_flux on the vertical axis
- We have also plotted two sets of lines
  - lines of constant β_t with α_t varied from 0 to 1 (green dashed lines)
  - lines of constant α_t, with β_t varied from 0 to 1 (blue solid lines)
- Plotting the experimentally determined combinations of F_DR and F_flux in this plane gives us estimates of the corresponding values of α_t and β_t

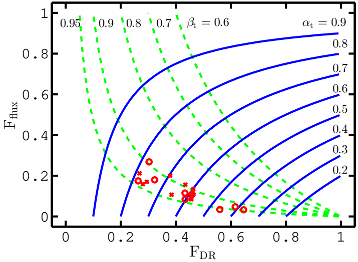

From Hajihoseini et al. (2019) *Plasma* **2** 201

Influence of magnetic field – α_{t} and β_{t}

- We can derive an equation that gives the back attraction probability β_{t} as a function of the measured quantities F_{flux} and F_{DR}
$$\beta_{\mathrm{t}} = \frac{1 - F_{\mathrm{DR}}}{1 - F_{\mathrm{DR}}(1 - F_{\mathrm{flux}})}$$
and similarly we can derive an equation that gives α_{t} as a function of the measured quantities
$$\alpha_{\mathrm{t}} = 1 - F_{\mathrm{DR}}(1 - F_{\mathrm{flux}}).$$

Influence of magnetic field – α_{t} *and* β_{t}

- When operating in the fixed voltage mode (**red**) the ionization probability α_{t} increases with increased magnetic field strength
- When operating in the fixed peak current mode (**black**) the ionization probability α_{t} is roughly constant independent of the magnetic field strength
- The back attraction probability is always high in the range 0.89 – 0.96 over the entire range of $B_{r,\mathrm{rt}}$

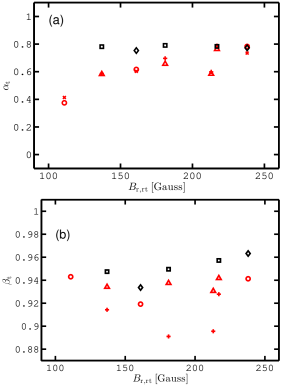

From Hajihoseini et al. (2019) *Plasma* 2 201

Influence of magnetic field – α_{t} and β_{t}

- In the fixed peak current mode (**black**) β_{t} increases slightly with increased $|\mathbf{B}|$ in the range 0.93 – 0.96 while α_{t} is almost constant in a narrow range 0.75 – 0.79
- If we assume a linear increase in β_{t} with $|\mathbf{B}|$ the fraction $(1-\beta_{\mathrm{t}})$ is roughly 30% higher at the highest $|\mathbf{B}|$ than at the lowest $|\mathbf{B}|$
- Recall that the total flux of ions of the sputtered material away from the target toward the substrate is $\Gamma_{\mathrm{DR,ions}} = \alpha_{\mathrm{t}}(1-\beta_{\mathrm{t}})\Gamma_0$

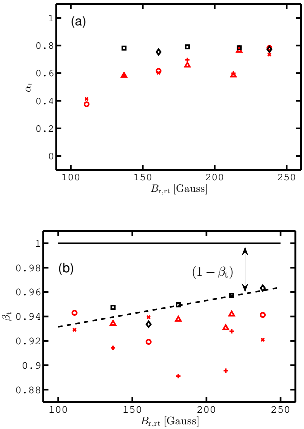

From Hajihoseini et al. (2019) *Plasma* **2** 201

Influence of magnetic field – Sideways deposition rate

- The ion meter was placed sideways over the target edge
- The ratio of the sideways deposition rate and the axial deposition rate
- Higher fraction of the sputtered species travels sideways in HiPIMS operation
- The sideways ionized flux fraction is in most cases significantly higher than the axial ionized flux fraction
- There appears to be no obvious trend with decreasing $|\mathbf{B}|$

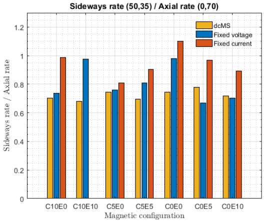

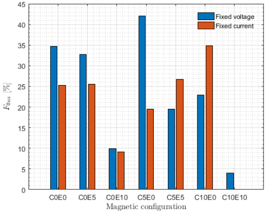

Summary

Summary

- For HiPIMS in the fixed voltage mode: A trade-off between the deposition rate (decreases by more than a factor of two) and the ionized flux fraction (increases by a factor 4 to 5) with increasing $|\mathbf{B}|$
- For HiPIMS in the fixed peak current mode: Decreasing $|\mathbf{B}|$ improves both the deposition rate (by 40%) and the ionized flux fraction (by 60%)
- When operating in the fixed peak current mode the ionization probability of the sputtered species is roughly constant while the parameter $(1-\beta_\mathrm{t})$ increases roughly 30% with decreasing $|\mathbf{B}|$
- When operating a HiPIMS discharge in fixed voltage mode the ionization probability α_t is varied by $|\mathbf{B}|$ and β_t remains roughly constant, while in the fixed peak current mode β_t varies with $|\mathbf{B}|$ and α_t remains roughly constant

Thank you for your attention

The slides can be downloaded at `http://langmuir.raunvis.hi.is/~tumi/ranns.html`

and the project is funded by

- Icelandic Research Fund Grant Nos. 130029, and 196141

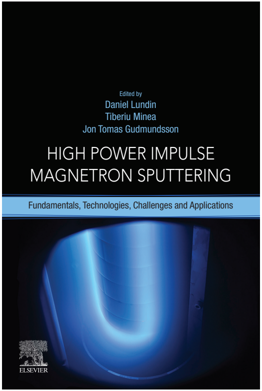

Edited by
Daniel Lundin
Tiberiu Minea
Jon Tomas Gudmundsson

HIGH POWER IMPULSE
MAGNETRON SPUTTERING

Fundamentals, Technologies, Challenges and Applications

ELSEVIER

- A comprehensive description of the HiPIMS process from the fundamental discharge physics to applications
- Shows how the HiPIMS process parameters can be adjusted to control film growth and thereby tune film properties, including hardness, refractive index, and residual stress

References

Alami, J., P. O. A. Petersson, D. Music, J. T. Gudmundsson, J. Bohlmark, and U. Helmersson (2005). Ion-assisted physical vapor deposition for enhanced film deposition on non-flat surfaces. *Journal of Vacuum Science and Technology A 23*(2), 278–280.

Anders, A., J. Andersson, and A. Ehiasarian (2007). High power impulse magnetron sputtering: Current-voltage-time characteristics indicate the onset of sustained self-sputtering. *J. Appl. Phys.* **102**(11), 113303.

Anders, A. (2008). Self-sputtering runaway in high power impulse magnetron sputtering: The role of secondary electrons and multiply charged metal ions. *Appl. Phys. Lett.* **92**(20), 201501.

Anders, A. (2010). Deposition rates of high power impulse magnetron sputtering: Physics and economics. *Journal of Vacuum Science and Technology A 28*(4), 783–790.

Bohlmark, J., J. Alami, C. Christou, A. P. Ehiasarian, and U. Helmersson (2005). Ionization of sputtered metals in high power pulsed magnetron sputtering. *Journal of Vacuum Science and Technology A 23*(1), 18–22.

Brenning, N., J. T. Gudmundsson, M. A. Raadu, T. J. Petty, T. Minea, and D. Lundin, (2017). A unified treatment of self-sputtering, process gas recycling, and runaway for high power impulse sputtering magnetrons. *Plasma Sources Sci. Technol.* **26**(12), 125003.

Butler, A., N. Brenning, M. A. Raadu, J. T. Gudmundsson, T. Minea, and D. Lundin (2018). On three different ways to quantify the degree of ionization in sputtering magnetrons. *Plasma Sources Science and Technology 27*(10), 105005.

DeKoven, B. M., P. R. Ward, R. E. Weiss, D. J. Christie, R. A. Scholl, W. D. Sproul, F. Tomasel, and A. Anders (2003). Carbon thin film deposition using high power pulsed magnetron sputtering. In *Society of Vacuum Coaters 46th Annual Technical Conference Proceedings*, San Francisco, CA, USA, pp. 158–165. Society of Vacuum Coaters.

Gudmundsson, J. T., N. Brenning, D. Lundin, and U. Helmersson (2012). The high power impulse magnetron sputtering discharge. *Journal of Vacuum Science and Technology A 30*(3), 030801.

Gudmundsson, J. T., D. Lundin, N. Brenning, M. A. Raadu, C. Huo, and T. M. Minea (2016). An ionization region model of the reactive Ar/O_2 high power impulse magnetron sputtering discharge. *Plasma Sources Science and Technology* **25**(6), 065004.

References

Hajihoseini, H., M. Čada, Z. Hubička, S. Ünaldi, M. A. Raadu, N. Brenning, J. T. Gudmundsson, and D. Lundin (2019). The effect of magnetic field strength and geometry on the deposition rate and ionized flux fraction in the HiPIMS discharge. *Plasma 2*(2), 201–221.

Helmersson, U., M. Lattemann, J. Bohlmark, A. P. Ehiasarian, and J. T. Gudmundsson (2006). Ionized physical vapor deposition (IPVD): A review of technology and applications. *Thin Solid Films 513*(1-2), 1–24.

Huo, C., D. Lundin, J. T. Gudmundsson, M. A. Raadu, J. W. Bradley, and N. Brenning (2017). Particle-balance models for pulsed sputtering magnetrons. *J. Phys. D: Appl. Phys.* **50**(35), 354003.

Huo, C., D. Lundin, M. A. Raadu, A. Anders, J. T. Gudmundsson, and N. Brenning (2014). On the road to self-sputtering in high power impulse magnetron sputtering: particle balance and discharge characteristics. *Plasma Sources Sci. Technol.* **23**(2), 025017.

Kateb, M., H. Hajihoseini, J. T. Gudmundsson, and S. Ingvarsson (2019). Role of ionization fraction on the surface roughness, density, and interface mixing of the films deposited by thermal evaporation, dc magnetron sputtering, and HiPIMS: An atomistic simulation. *Journal of Vacuum Science and Technology A 37*(3), 031306.

Kouznetsov, V., K. Macák, J. M. Schneider, U. Helmersson, and I. Petrov (1999). A novel pulsed magnetron sputter technique utilizing very high target power densities. *Surface and Coatings Technology 122*(2-3), 290–293.

Kubart, T., M. Čada, D. Lundin, and Z. Hubička (2014). Investigation of ionized metal flux fraction in HiPIMS discharges with Ti and Ni targets. *Surface and Coatings Technology 238*, 152–157.

Lundin, D., M. Čada, and Z. Hubička (2015). Ionization of sputtered Ti, Al, and C coupled with plasma characterization in HiPIMS. *Plasma Sources Science and Technology 24*(3), 035018.

Macak, K., V. Kouznetsov, J. Schneider, U. Helmersson, and I. Petrov (2000). Ionized sputter deposition using an extremely high plasma density pulsed magnetron discharge. *Journal of Vacuum Science and Technology A 18*(4), 1533 – 1537.

Samuelsson, M., D. Lundin, J. Jensen, M. A. Raadu, J. T. Gudmundsson, and U. Helmersson (2010). On the film density using high power impulse magnetron sputtering. *Surface and Coatings Technology 202*(2), 591–596.

Vlček, J. and K. Burcalová (2010). A phenomenological equilibrium model applicable to high-power pulsed magnetron sputtering. *Plasma Sources Science and Technology 19*(6), 065010.